The corticothalamocortical circuit drives higher-order cortex in the mouse

Brian B Theyel[1], Daniel A Llano[2,3] & S Murray Sherman[1]

An unresolved question in neuroscience relates to the extent to which corticothalamocortical circuits emanating from layer 5B are involved in information transfer through the cortical hierarchy. Using a new form of optical imaging in a brain slice preparation, we found that the corticothalamocortical pathway drove robust activity in higher-order somatosensory cortex. When the direct corticocortical pathway was interrupted, secondary somatosensory cortex showed robust activity in response to stimulation of the barrel field in primary somatosensory cortex (S1BF), which was eliminated after subsequently cutting the somatosensory thalamus, suggesting a highly efficacious corticothalamocortical circuit. Furthermore, after chemically inhibiting the thalamus, activation in secondary somatosensory cortex was eliminated, with a subsequent return after washout. Finally, stimulation of layer 5B in S1BF, and not layer 6, drove corticothalamocortical activation. These findings suggest that the corticothalamocortical circuit is a physiologically viable candidate for information transfer to higher-order cortical areas.

Much of neocortex can be divided into macroscopic zones: visual, auditory and somatomotor. Each of these is comprised of a number of discrete areas[1–3] that function together to analyze relevant information (for example, visual, etc.). An important first step toward understanding how cortex functions is to elucidate the manner in which information flows between these discrete cortical areas. The prevailing dogma[4–6] is that this flow of information is subserved by direct corticocortical pathways. In the visual system, for example, this implies that once information reaches primary visual cortex from the lateral geniculate nucleus, it remains exclusively in cortex as it flows up the cortical hierarchy. In this scheme, beyond relaying the initial information to cortex (for example, the geniculocortical pathway), the thalamus is not involved beyond modulation of corticocortical information flow[6]. However, a recent hypothesis suggests that much, and perhaps the vast majority of, information flow between cortical areas involves higher-order thalamic nuclei in the form of corticothalamocortical circuits[7–9].

This latter hypothesis is based partly on the idea that many brain circuits can be divided into 'drivers', which represent the main information routes, and 'modulators', which serve to modulate information flow[10,11]. Well-documented examples of drivers are the retinal input to the lateral geniculate nucleus or lemniscal input to the ventral posterior nucleus; modulator examples are feedback layer 6 corticothalamic projections and cholinergic brainstem inputs to thalamus[10–14]. In this context, the information route involving driver corticothalamocortical circuits emanates from layer 5B cells, initiating a feedforward thalamocortical circuit[1,12], as opposed to the modulating, feedback layer 6 corticothalamic pathway. Although the aforementioned evidence, in aggregate, is suggestive of a highly efficacious corticothalamocortical circuit, no study has directly tested its ability to activate cortex.

We found that, based on activity of circuits evoked in slices of the mouse brain, a corticothalamocortical circuit starting in S1BF strongly activates secondary somatosensory cortex. This finding suggests that corticothalamocortical pathways are powerful enough to carry receptive field–defining information to higher-order cortical areas.

RESULTS

The mouse thalamocortical somatosensory slice[2] contains much of the somatosensory corticothalamocortical circuit (**Fig. 1**). The relevant structures in the slice include S1BF, secondary somatosensory cortex, posterior medial nucleus of the thalamus (POm), and the connections between S1BF/POm and secondary somatosensory cortex/POm[1,2,15–17]. To anatomically verify this connectivity, we placed a retrograde tracer (1,1′-dioctadecyl-3,3,3′3′-tetramethylindocarbocyanine perchlorate) into the upper layers (layers 2/3 and 4) of secondary somatosensory cortex in the same type of slice used for our experiments. Retrogradely-labeled cells were observed in POm, anatomically confirming that these connections remained. We primarily employed flavoprotein autofluorescence imaging[18,19] to assess whether the corticothalamocortical circuit could drive secondary somatosensory cortex responses.

Cut sequence

After verifying flavoprotein autofluorescence activity in both secondary somatosensory cortex and thalamus following electrical stimulation of layer 5B in S1BF, we identified the border between S1BF and secondary somatosensory cortex by locating the abrupt disappearance of barrels, which were visible under both brightfield and fluorescence illumination. We confirmed that this was the correct location using an atlas and nearby characteristic landmarks[20]. We then used a bent syringe needle to make a radial cut between the stimulation site in
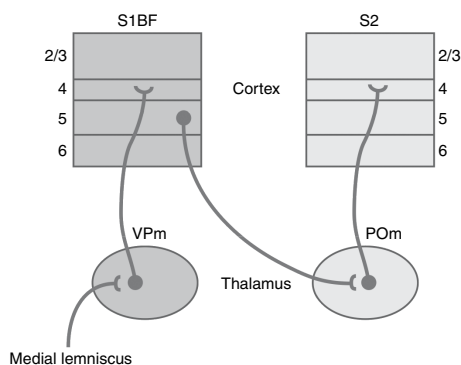
Figure 1 Line drawing of the corticothalamocortical circuit. The corticothalamocortical circuit emanates from layer 5B, which contains pyramidal cells that send excitatory projections to relay cells in a higher-order area of the thalamus. These higher-order thalamic relay cells then project to layer 4 of higher-order cortex, similar to the first-order ascending pathway (shown on the left). Dark grey indicates first order and light grey indicates higher order. S2, secondary somatosensory cortex.

S1BF and secondary somatosensory cortex that extended into the white matter, thereby severing the direct corticocortical afferents connecting them (see Online Methods). After making the cut, we stimulated S1BF at the same location that we used for the first stimulus. In three slices, activity in secondary somatosensory cortex and POm remained despite the ablation of the direct corticocortical pathway (**Fig. 2** and **Supplementary Video 1**). $\Delta F/F$ was slightly decreased in secondary somatosensory cortex in all three slices and was not significantly different in POm compared to activity levels before the cut. We then made a second cut across the dorsolateral aspect of ventroposteriomedial nucleus of the thalamus (VPm) and POm, ensuring the disruption of all thalamic projections to secondary somatosensory cortex (**Fig. 2c**). S1BF stimulation following this cut failed to activate secondary somatosensory cortex in all three slices. To ensure that the cut eliminated any possibility of activating secondary somatosensory cortex, we increased the stimulus amplitude sixfold during one of our experiments and were still unable to observe any appreciable secondary somatosensory cortex activity after the second cut.

These data suggest that direct corticocortical projections are not necessary to activate secondary somatosensory cortex in these slices and that a corticothalamocortical circuit is capable of doing so. Several other circuits could conceivably be responsible for this activation following direct corticocortical disruption. It is possible that branched collaterals of thalamic relay cell axons that innervate both S1BF and secondary somatosensory cortex[21] were antidromically activated, leading to orthrodromic thalamocortical activation of secondary somatosensory cortex. Another possibility is that the cut may not have completely severed corticocortical axons. Finally, an unknown pathway could be involved.

Reversible inhibition

To ensure that corticothalamocortical circuit activation and deactivation accounted for changes in secondary somatosensory cortex activity, we undertook a series of experiments using both glutamate stimulation, which avoids axonal activation, and selective, reversible blockade of thalamus using a focal injection of 6,7-dinitroquinoxaline-2,3-dione (DNQX). In these experiments, we imaged flavoprotein autofluorescence fluctuations while stimulating before, during and then after DNQX application to thalamus (see Online Methods, **Fig. 3** and **Supplementary Videos 2** and **3**). We performed these experiments in nine slices, each from a different mouse (**Fig. 3b**). The maximal

secondary somatosensory cortex $\Delta F/F$ values were decreased by 89.8 $\pm$ 4.5% during runs with maximal thalamic inactivation ($n = 9$, $P = 0.0007$, paired t test). Furthermore, $\Delta F/F$ values after DNQX washout were not significantly different from baseline ($n = 9$, $P = 0.33$, paired t test), indicating that there was a full recovery in secondary somatosensory cortex. These data suggest that the corticothalamocortical pathway is a potent activator of secondary somatosensory cortex.

To determine whether the DNQX injection reached S1BF or secondary somatosensory cortex, which could have directly inhibited secondary somatosensory cortex activation, we injected a fluorescent tracer (Texas Red 10,000 molecular-weight lysine-fixable dextran, Invitrogen) into the thalamus using the same protocol that we used to inject DNQX (**Fig. 3f** and **Supplementary Video 3**). We monitored an entire 6-min injection to ensure that the injection medium did not reach cortex. It was clear from the video that the injection stream did not approach S1BF or secondary somatosensory cortex. A further indication that the DNQX did not affect the relevant parts of cortex was the stability of upper layer activation in the column that we stimulated throughout all runs (**Fig. 3**).

During three of the runs, we recorded from a single neuron in the upper layers of secondary somatosensory cortex using whole-cell patch clamp throughout the entire manipulation, providing electrophysiological verification of the imaging results (**Fig. 4**). Recordings from each of these three cells and the corresponding flavoprotein autofluorescence signals were well-aligned with one another, as was expected given the previously described correlations between flavoprotein autofluorescence signal strength in the neocortex and underlying physiological activity[22]. Before applying DNQX to the thalamus, we observed a strong optical signal in secondary somatosensory cortex following S1BF stimulation and a correspondingly robust inward synaptic current in a neuron recorded in the region of the flavoprotein autofluorescence response. After DNQX application, both the optical and electrophysiological signals were abolished and both returned after subsequent washout of DNQX. Cellular activity, similar to the aforementioned flavoprotein autofluorescence imaging results, decreased by 91.73 $\pm$ 0.47% during

Figure 2 Demonstration of corticothalamocortical pathway sufficiency to drive secondary somatosensory cortex activity: electrical stimulation. Shown are $\Delta F/F$ (change in fluorescence/baseline fluorescence) images overlaid on top of raw images for anatomy. Insets are optical traces for the region delineated by the blue circles in secondary somatosensory cortex. The images depict a single cut-sequence experiment (total $n = 3$). (**a**) Secondary somatosensory cortex response to S1BF stimulation in a somatosensory slice preparation. (**b**) Secondary somatosensory cortex response following a cut between S1 and secondary somatosensory cortex. $\Delta F/F$ was decreased by 45.5% in secondary somatosensory cortex and 11.6% in POm compared with baseline. (**c**) Cortical response following thalamic ablation (**Supplementary Video 1**). $\Delta F/F$ was decreased by 81.6% in secondary somatosensory cortex and 92.7% in POm compared with baseline.
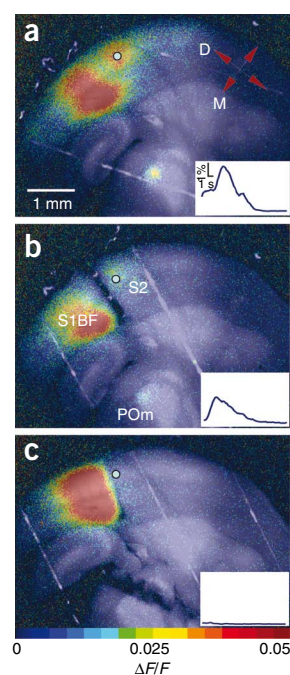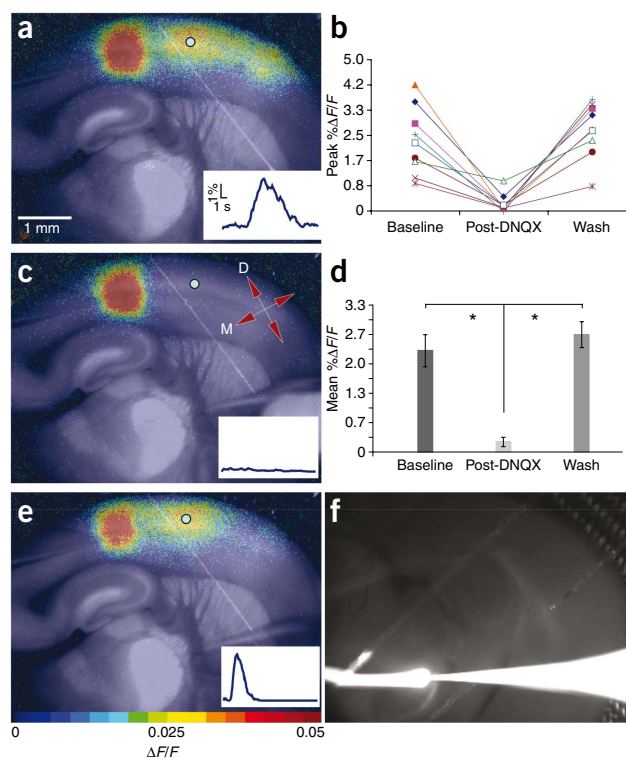
Figure 3 Demonstration of corticothalamocortical pathway sufficiency to drive secondary somatosensory cortex activity: reversible inactivation. (**a**) Stimulation of layer 5B of S1BF via microspritzing of glutamate (see Online Methods). (**b**) Maximum percent $\Delta F/F$ before, during and after DNQX treatment (all runs are shown). We chose 5×5 pixel (83×83 μm) regions of interest in secondary somatosensory cortex for each trial. These regions were analyzed to determine maximal $\Delta F/F$ values during the baseline run (before DNQX), post-DNQX run and washout. The values for all nine experiments are plotted. (**c**) Slice response to the same stimulus used in **a** ~4 min after local application of 500 μM DNQX in the thalamic hotspot. D, dorsal; M, medial. (**d**) Mean percent $\Delta F/F$ before, during and after DNQX inactivation of thalamus (baseline, 2.29 ± 0.36%; post-DNQX, 0.2 ± 0.10%; wash, 2.66 ± 0.30%; see **Supplementary Video 2**). The data shown in **b** were averaged and compared using a two-tailed t test. An asterisk indicates a significant difference; baseline and post-DNQX, $n = 9$, $P = 0.0007$; post-DNQX and wash, $n = 9$, $P = 0.00008$ (see Results and Online Methods). Error bars indicate s.e.m. (**e**) Flavoprotein autofluorescence activity in response to same stimulus used in **a** and **c** after DNQX washout. (**f**) Injection spread control. We injected a fluorescent tracer into the thalamus using the same procedure that we used while injecting DNQX. The white line extending left from the electrode tip is the tracer stream. Artificial cerebrospinal fluid (ACSF) flowed from right to left (**Supplementary Video 3**).

successful DNQX trials for the three cells, each of which were from separate experiments ($n = 3$, $P = 0.000026$, paired t test). We lost one cell while removing the DNQX pipette, but the remaining two cells regained much of their previous activation. Similar to statistical data for the optical analyses described above, single-cell activity returned to baseline levels after wash.

Corticothalamocortical circuit verification

We sought to ensure that activation in our slices originated in layer 5B, the layer of origin for the corticothalamocortical circuit, and not layer 6, which sends feedback to the thalamus. We pressure-injected glutamate into S1BF in somatosensory slices from two mice starting in layer 5B and steadily moved the stimulation site toward the white matter until the corticothalamocortical circuit was no longer activated. We found that stimulation of layer 6, which sends modulatory afferents to thalamus[10,12], did not activate secondary somatosensory cortex via this circuit. Subsequent stimuli in layer 5B elicited secondary somatosensory cortex activation, verifying that the circuit was still viable after the failures of the layer 6 stimulations. We also carried

Figure 4 Simultaneous flavoprotein autofluorescence imaging and whole-cell recording in secondary somatosensory cortex. (**a**–**c**) Shown are optical traces along with voltage-lamp recordings from a representative (one of three) neuron in secondary somatosensory cortex before (**a**), ~6 min after (**b**) and ~12 min after (**c**) local DNQX application to thalamus. Optical traces and intracellular recordings were consistent (no cellular activity in conditions of no optical activity) and temporally synchronized at onset.

out this sequence in a slice from another mouse with low levels of electrical stimulation (2 μA, see Online Methods for stimulus train parameters) and obtained similar results.

To confirm that stimulation in S1BF was generating suprathreshold activity in the thalamus, we recorded extracellularly from six POm neurons in three somatosensory slices (two neurons each) in a loose seal configuration while photostimulating in S1BF. We observed spiking activity in 2 out of 6 cells from a single slice with an average of 3.64 ± 0.49 spikes elicited per stimulus (**Supplementary Fig. 1**). We also used extracellular recording electrodes in open configuration (described in Online Methods) to record multiunit activity from POm in three other slices. We found reliable multiunit spiking activity that was time-locked to stimulation in S1BF in each slice (**Supplementary Fig. 1**). These data indicate that glutamate stimulation in the corticothalamocortical slices that we used was able to drive spiking in POm, a requisite for corticothalamocortical circuit activation. Furthermore, when photostimulating in layer 6 of S1BF with the same stimulus, both neurons in the loose-seal configuration failed to spike, also suggesting that layer 5B, rather than layer 6, corticothalamic afferents were responsible for the activation of the corticothalamocortical pathway in our slice preparations.

DISCUSSION

Previous work indicates that individual elements in the corticothalamocortical circuit have driver properties. Layer 5B inputs to POm are of large diameter, contact proximal dendrites and have synaptic properties that are consistent with driver inputs[12,23]. In addition, receptive fields in POm depend on S1BF input[24]. Furthermore, activation of the higher-order thalamocortical projection from POm to secondary somatosensory cortex elicits synaptic responses that are characteristic of driver input[1]. Here we have demonstrated the efficacy of the entire circuit by providing evidence that a substantial proportion of the secondary somatosensory cortex activation in our slices depended on thalamic circuitry. Given that our results came from experiments on brain slices with many cut connections, it is
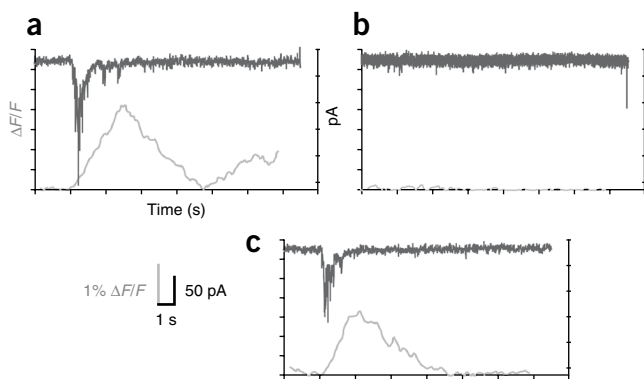
likely that the corticothalamocortical circuit is highly efficacious in an intact mouse, although this will need verification.

We have found for the first time, to the best of our knowledge, that a corticothalamocortical circuit involving POm provides a strong connection between S1BF and secondary somatosensory cortex. A question that remains unresolved is the efficacy of the direct S1BF to secondary somatosensory cortex pathway. Although we found little evidence regarding the strength of this pathway, we believe that this may be an artifact of our slice, which was optimized for thalamocortical and corticothalamic circuits. Indeed, other evidence[15] indicates that direct corticocortical connections are mostly cut in this preparation. Thus, we emphasize that what we have found here is a strong, hitherto unexplored, corticothalamocortical circuit, and this is the main point of this investigation. A proper comparison with the direct S1 to secondary somatosensory cortex circuit must await further study.

Before the hypothesis that much of the information transfer between cortical areas involves corticothalamocortical circuits can be accepted, our findings will need to be generalized to other sensory systems *in vitro* (if possible) and *in vivo*. We should note that there is evidence supporting the existence of multiple key features of corticothalamocortical driving circuitry in the visual and auditory systems, including driver-like corticothalamic inputs from layer 5B[25–31], higher-order thalamic receptive-field dependency on cortical inputs[24,32] and nonreciprocal corticothalamocortical organization for layer 5B, but not layer 6, corticothalamic outputs[33–35]. The presence of similar circuitry in other sensory systems, in combination with our results, suggests that corticothalamocortical information transfer may represent an important addition to, or even replacement of, the current dogma that corticocortical transfer of primary information exclusively involves direct corticocortical pathways.

The corticothalamocortical hypothesis also raises questions about the utility of thalamic circuitry in information processing. Just as there is no a priori reason for information to pass through the thalamus from the sensory periphery to the cortex, there is no obvious reason for an additional thalamic pathway between cortical areas. Furthermore, the presence of corticothalamocortical driving pathways leaves open the question of the nature of the ubiquitous direct corticocortical pathways. Are they modulatory, driving, a combination of the two or something else entirely? Although this will require further study, the possibility or even likelihood that these direct corticocortical pathways do indeed provide another route of information flow would suggest a system of two parallel streams of information: corticocortical and corticothalamocortical. A major difference between these routes might be related to the observation that, although essentially all direct corticocortical projections lie strictly in cortex, the corticothalamocortical pathway emanates from layer 5B cells, most or all of which have axons that branch to innervate thalamus and other subcortical structures that appear to be mostly motor in nature[36–38]. Thus, this arm of information transfer reflects output that is sent to both cortical and extrathalamic subcortical motor targets, implying that this circuit, by having a large effect on its cortical target, may be an effective monitor of motor control signals[39].

METHODS

Methods and any associated references are available in the online version of the paper at http://www.nature.com/natureneuroscience/.

Note: Supplementary information is available on the Nature Neuroscience website.

AUTHOR CONTRIBUTIONS
B.B.T. performed all of the experimental manipulations and data analysis.
All authors contributed to hypothesis development, experimental design, data interpretation and manuscript preparation.

1. Lee, C.C. & Sherman, S.M. Synaptic properties of thalamic and intracortical inputs to layer 4 of the first- and higher-order cortical areas in the auditory and somatosensory systems. *J. Neurophysiol.* **100**, 317–326 (2008).
2. Agmon, A. & Connors, B.W. Thalamocortical responses of mouse somatosensory (barrel) cortex *in vitro*. *Neuroscience* **41**, 365–379 (1991).
3. Cox, C.L. & Sherman, S.M. Control of dendritic outputs of inhibitory interneurons in the lateral geniculate nucleus. *Neuron* **27**, 597–610 (2000).
4. Kaas, J.H. The organization of neocortex in mammals: implications for theories of brain function. *Annu. Rev. Psychol.* **38**, 129–151 (1987).
5. Van Essen, D.C., Anderson, C.H. & Felleman, D.J. Information processing in the primate visual system: an integrated systems perspective. *Science* **255**, 419–423 (1992).
6. Olshausen, B.A., Anderson, C.H. & Van Essen, D.C. A neurobiological model of visual attention and invariant pattern recognition based on dynamic routing of information. *J. Neurosci.* **13**, 4700–4719 (1993).
7. Sherman, S.M. & Guillery, R.W. The role of the thalamus in the flow of information to the cortex. *Philos. Trans. R. Soc. Lond. B Biol. Sci.* **357**, 1695–1708 (2002).
8. Guillery, R.W. & Sherman, S.M. Thalamic relay functions and their role in corticocortical communication: generalizations from the visual system. *Neuron* **33**, 163–175 (2002).
9. Sherman, S.M. Thalamic relay functions. *Prog. Brain Res.* **134**, 51–69 (2001).
10. Sherman, S.M. & Guillery, R.W. On the actions that one nerve cell can have on another: distinguishing drivers from modulators. *Proc. Natl. Acad. Sci. USA* **95**, 7121–7126 (1998).
11. Sherman, S.M. & Guillery, R.W. Functional organization of thalamocortical relays. *J. Neurophysiol.* **76**, 1367–1395 (1996).
12. Reichova, I. & Sherman, S.M. Somatosensory corticothalamic projections: distinguishing drivers from modulators. *J. Neurophysiol.* **92**, 2185–2197 (2004).
13. Wilson, J.R., Friedlander, M.J. & Sherman, S.M. Fine structural morphology of identified X- and Y-cells in the cat's lateral geniculate nucleus. *Proc. R. Soc. Lond. B* **221**, 411–436 (1984).
14. Sherman, S.M. & Guillery, R.W. *Exploring the Thalamus and its Role in Cortical Function* (The MIT Press, Cambridge, Massachusetts, 2006).
15. Staiger, J.F., Kötter, R., Zilles, K. & Luhmann, H.J. Connectivity in the somatosensory cortex of the adolescent rat: an *in vitro* biocytin study. *Anat. Embryol. (Berl.)* **199**, 357–365 (1999).
16. MacLean, J.N., Fenstermaker, V., Watson, B.O. & Yuste, R. A visual thalamocortical slice. *Nat. Methods* **3**, 129–134 (2006).
17. Cruikshank, S.J., Rose, H.J. & Metherate, R. Auditory thalamocortical synaptic transmission *in vitro*. *J. Neurophysiol.* **87**, 361–384 (2002).
18. Reinert, K.C., Dunbar, R.L., Gao, W., Chen, G. & Ebner, T.J. Flavoprotein autofluorescence imaging of neuronal activation in the cerebellar cortex *in vivo*. *J. Neurophysiol.* **92**, 199–211 (2004).
19. Shibuki, K. *et al.* Dynamic imaging of somatosensory cortical activity in the rat visualized by flavoprotein autofluorescence. *J. Physiol. (Lond.)* **549**, 919–927 (2003).
20. Franklin, K.B.J.P.G. *The Mouse Brain in Stereotaxic Coordinates* (Academic Press, San Diego, California, 2008).
21. Spreafico, R., Barbaresi, P., Weinberg, R.J. & Rustioni, A. SII-projecting neurons in the rat thalamus: a single- and double-retrograde-tracing study. *Somatosens. Res.* **4**, 359–375 (1987).
22. Llano, D.A., Theyel, B.B., Mallik, A.K., Sherman, S.M. & Issa, N.P. Rapid and sensitive mapping of long-range connections *in vitro* using flavoprotein autofluorescence imaging combined with laser photostimulation. *J. Neurophysiol.* **101**, 3325–3340 (2009).
23. Groh, A., de Kock, C.P.J., Wimmer, V.C., Sakmann, B. & Kuner, T. Driver or coincidence detector: modal switch of a corticothalamic giant synapse controlled by spontaneous activity and short-term depression. *J. Neurosci.* **28**, 9652–9663 (2008).
24. Diamond, M.E., Armstrong-James, M., Budway, M.J. & Ebner, F.F. Somatic sensory responses in the rostral sector of the posterior group (POm) and in the ventral posterior medial nucleus (VPM) of the rat thalamus: dependence on the barrel field cortex. *J. Comp. Neurol.* **319**, 66–84 (1992).
25. Mathers, L.H. The synaptic organization of the cortical projection to the pulvinar of the squirrel monkey. *J. Comp. Neurol.* **146**, 43–60 (1972).
26. Guillery, R.W., Feig, S.L. & Van Lieshout, D.P. Connections of higher order visual relays in the thalamus: a study of corticothalamic pathways in cats. *J. Comp. Neurol.* **438**, 66–85 (2001).

27. Rouiller, E.M. & Welker, E. Morphology of corticothalamic terminals arising from the auditory cortex of the rat: a *Phaseolus vulgaris* leucoagglutinin (PHA-L) tracing study. *Hear. Res.* **56**, 179–190 (1991).

28. Ojima, H. Terminal morphology and distribution of corticothalamic fibers originating from layers 5 and 6 of cat primary auditory cortex. *Cereb. Cortex* **4**, 646–663 (1994).

29. Bajo, V.M. *et al.* Morphology and spatial distribution of corticothalamic terminals originating from the cat auditory cortex. *Hear. Res.* **83**, 161–174 (1995).

30. Winer, J.A., Larue, D.T. & Huang, C.L. Two systems of giant axon terminals in the cat medial geniculate body: convergence of cortical and GABAergic inputs. *J. Comp. Neurol.* **413**, 181–197 (1999).

31. Hazama, M., Kimura, A., Donishi, T., Sakoda, T. & Tamai, Y. Topography of corticothalamic projections from the auditory cortex of the rat. *Neuroscience* **124**, 655–667 (2004).

32. Bender, D.B. Visual activation of neurons in the primate pulvinar depends on cortex, but not colliculus. *Brain Res.* **279**, 258–261 (1983).

33. Van Horn, S.C. & Sherman, S.M. Differences in projection patterns between large and small corticothalamic terminals. *J. Comp. Neurol.* **475**, 406–415 (2004).

34. Llano, D.A. & Sherman, S.M. Evidence for nonreciprocal organization of the mouse auditory thalamocortical-corticothalamic projection systems. *J. Comp. Neurol.* **507**, 1209–1227 (2008).

35. Kato, N. Cortico-thalamo-cortical projection between visual cortices. *Brain Res.* **509**, 150–152 (1990).

36. Bourassa, J. & Deschênes, M. Corticothalamic projections from the primary visual cortex in rats: a single fiber study using biocytin as an anterograde tracer. *Neuroscience* **66**, 253–263 (1995).

37. Bourassa, J., Pinault, D. & Deschenes, M. Corticothalamic projections from the cortical barrel field to the somatosensory thalamus in rats: a single-fibre study using biocytin as an anterograde tracer. *Eur. J. Neurosci.* **7**, 19–30 (1995).

38. Guillery, R.W. Branching thalamic afferents link action and perception. *J. Neurophysiol.* **90**, 539–548 (2003).

39. Guillery, R.W. & Sherman, S.M. The thalamus as a monitor of motor outputs. *Phil. Trans. R. Soc. Lond. B* **357**, 1809–1821 (2002).

ONLINE METHODS

We obtained somatosensory slices[2] from male and female mice (BALB/c *Mus musculus*, 12–22 d) using standard, previously published techniques[1] with only minor variations. All procedures were approved by the Institutional Animal Care and Use Committee at the University of Chicago. We first anesthetized the mice (Harlan Sprague-Dawley) with a mixture of 1 mg per kg of body weight ketamine (Vetaket, Phoenix Scientific) and 10 mg per kg xylazine, and, after the hindlimb reflex was absent, perfused them with chilled (~4 °C) sucrose-based slicing solution[1] before cutting. After cutting, we transferred the slices to a holding chamber containing oxygenated ACSF consisting of 26 mM NaHCO$_3$, 2.5 mM KCl, 10 mM glucose, 126 mM NaCl, 1.25 mM NaH$_2$PO$_4$*H$_2$O, 3 mM MgCl$_2$*6H$_2$O and 1.1. mM CaCl$_2$*2H$_2$O, where they incubated for at least 1 h before imaging/recording.

We implemented whole-cell patch-clamp recordings (**Fig. 4**) using standard, previously described techniques[3,12,40–42]. We monitored the access resistance of the cells throughout the recordings, which lasted >1 h for most experiments, and only included neurons with a stable access of less than 30 MΩ in our analysis.

We performed extracellular recordings in either a loose seal or open configuration. For loose-seal recordings, we placed 4–6 MΩ glass pipettes filled with ACSF adjacent to a neuronal cell membrane and applied a slight amount of negative pressure to achieve ~500 MΩ to 1 GΩ for recordings. In open configuration, we lowered broken back glass electrodes (~5–10 μm) ~50–100 μm into the tissue (POm). To detect spikes, we used manual thresholding in Clampfit (Molecular Devices) and used the resulting spike times to construct peristimulus time histograms in Excel (Microsoft). We set thresholds well above baseline noise conditions and visually confirmed that the waveforms were consistent with that of an action potential.

We were able to easily identify POm in slices as a thalamic region that had a lighter appearance than the neighboring VPm under brightfield illumination; we distinguished S1BF from secondary somatosensory cortex by the barrels and septa that were resolved in the former. We identified the approximate borders between cortical layers in S1BF (and often in secondary somatosensory cortex) using the following criteria. Layer 4 contained characteristic barrel structures and a relative dark contrast compared with layer 5A, which appeared as a light-color band under bright-field illumination. Layer 5B was differentiated from the neighboring layer 5A and layer 6, even at low magnification, by the presence of a large number of loosely packed large cell bodies that formed a dark strip under brightfield illumination.

Thalamic inhibition. For irreversible circuit inactivation (**Fig. 3**), we made radial cuts with a bent syringe needle (27.5 gauge) attached to a micromanipulator between S1 and secondary somatosensory cortex, extending through the subcortical white matter to eliminate the direct corticocortical pathway. We then made another cut between VPm and the thalamic reticular nucleus to sever fibers between POm and cortex, thus eliminating the corticothalamocortical circuit. We waited at least 30 min after each cut to assess slice activity. For reversible thalamic inactivation, we focally injected ~15 μL 500 μM DNQX in ACSF using a glass micropipette (5–10 μm) over the course of ~7 min into an area just adjacent to the thalamic hotspot to avoid damaging relevant thalamic relay cells. We used this method to locally deactivate the circuit without directly affecting cortical activity. For these experiments, we first assessed circuit activation in each slice by microspritzing glutamate or photostimulating via photolysis of glutamate (see Online Methods) in layer 5B of S1BF. After we observed activation in both POm and secondary somatosensory cortex, we locally applied 500 μM DNQX to the thalamic hotspot with a micropipette (~5–10 μm diameter) over the course of 6–7 min. After applying DNQX, we stimulated the circuit once every 2 min. If two or more failures of secondary somatosensory cortex activation (assessed by visual inspection of ΔF/F data) occurred that were followed by the return of circuit activation within 20 min of the DNQX application, we deemed the run a successful deactivation and subsequent reactivation of the corticothalamocortical circuit.

Stimulation. For the electrical-stimulation experiments (**Fig. 2**), we delivered 20-Hz, 1-s-long trains of 10-ms pulses at varying amplitudes before and after each cut using a glass pipette (5–10 μm diameter) filled with ACSF. We delivered a 30-μA stimulus for the baseline run and for the cortical cut run. After the thalamic cut, we used a 150-μA train to further illustrate that secondary somatosensory cortex was no longer being activated. During reversible experiments,

we used photostimulation (one experiment) and pressure injection of glutamate (eight experiments). The photostimulation techniques have been previously described[40,43]. We delivered a 20-Hz, 200-ms-long train of 10-ms pulses at 60-mA laser power to Layer 5B of S1BF or injected glutamate using a 20-Hz, 1-s-long train of 10-ms pulses at ~4–6 psi using a glass pipette filled with 10 μM L-glutamate in ACSF. We stimulated before DNQX application and then again after DNQX application at 2-min intervals until secondary somatosensory cortex signal elimination and subsequent recovery had occurred. If obvious secondary somatosensory cortex deactivation was not achieved, we stopped collecting data 20 min after DNQX application. We used our previously described methods for photostimulation[40–42]. In past experiments, we and others[43,44] found no change of the recording quality or large tissue response changes during photostimulation experiments that might suggest damage from phototoxicity.

Flavoprotein autofluorescence imaging. We performed flavoprotein autofluorescence imaging (**Figs. 2**–**4**) as previously described[22]. We captured green light (520–560 nm) generated by mitochondrial flavoproteins in the presence of blue light (472–488 nm) using a high sensitivity camera (QImaging Retiga-SRV, QImaging) with a Firewire interface. We acquired all images using 4 × 4 binning at 8 bits with 2.5× magnification. Final image resolution was 348 × 260 pixels, with 60 pixels spanning 1 mm in both the *x* and *y* dimensions. We suspended slices above the chamber bottom with a piece of titanium mesh mounted on a hand-bent platinum wire to maintain adequate slice oxygenation and perfusion on both sides of the slice. This has been shown by others[19], and in our experience, to substantially increase the flavoprotein autofluorescence signal amplitude. We typically captured images for 14-s-long sweeps, with stimuli occurring during the second second of each sweep. We stored the resulting images on a custom-built computer running a commercially available software package (Streampix 3, Norpix) and analyzed them with programs that we generated to run on Matlab (Mathworks). In the case of simultaneous whole-cell recordings (**Fig. 4**), we selected a box of pixels located immediately over the group of cells near the electrode tip in ImageJ (US National Institutes of Health) and exported them to Excel, where we produced line graphs.

We typically acquired flavoprotein autofluorescence images at a rate of 7–12 frames per s. We manually adjusted exposure times to yield image brightness (that is, baseline flavoprotein autofluorescence) that was subjectively similar across experiments. After acquisition and processing (details above), we uniformly adjusted the contrast, brightness and transparency of flavoprotein autofluorescence images and then overlaid onto raw images from Streampix 3 in CorelDRAW X4 (Corel).

Statistics. We used a two-tailed *t* test to determine the significance of the DNQX runs (**Fig. 3**). To obtain baseline condition data, we used maximal ΔF/F values for baseline runs, runs after DNQX application and runs after we washed out DNQX by selecting a 5 × 5 pixel box over layer 4 in secondary somatosensory cortex in ImageJ and subtracting another set of ΔF/F values obtained from a 5 × 5 pixel in an area in which we observed no activity (the same method was used in the cut experiment). This helped to control for photobleaching and uniform noise. We analyzed runs with the maximal decrease in ΔF/F after DNQX application for the post-DNQX condition in each experiment.

We translated whole-cell recording data (currents) into area (pA × ms) for 2.5-s windows beginning at the stimulus onset. The post-DNQX run and wash run were normalized to the baseline condition for each experiment and were compared using paired *t* tests.

40. Lam, Y.-W. & Sherman, S.M. Mapping by laser photostimulation of connections between the thalamic reticular and ventral posterior lateral nuclei in the rat. *J. Neurophysiol.* **94**, 2472–2483 (2005).
41. Lam, Y.-W., Nelson, C.S. & Sherman, S.M. Mapping of the functional interconnections between thalamic reticular neurons using photostimulation. *J. Neurophysiol.* **96**, 2593–2600 (2006).
42. Lam, Y.-W. & Sherman, S.M. Different topography of the reticulothalamic inputs to first- and higher-order somatosensory thalamic relays revealed using photostimulation. *J. Neurophysiol.* **98**, 2903–2909 (2007).
43. Shepherd, G.M.G., Pologruto, T.A. & Svoboda, K. Circuit analysis of experience-dependent plasticity in the developing rat barrel cortex. *Neuron* **38**, 277–289 (2003).
44. Callaway, E.M. & Katz, L.C. Photostimulation using caged glutamate reveals functional circuitry in living brain slices. *Proc. Natl. Acad. Sci. USA* **90**, 7661–7665 (1993).